Supplementary Information for

Multi-year black carbon observations and modeling close to the largest gas flaring and wildfire regions (Western Siberian Arctic)

Olga B. Popovicheva[1], Marina A. Chichaeva[2], Nikolaos Evangeliou[3], Sabine Eckhardt[3], Evangelia Diapouli[4], and Nikolay S. Kasimov[2]

[1]SINP, Lomonosov Moscow State University, 119991 Moscow, Russia

[2] Faculty of Geography, Lomonosov Moscow State University, 119991 Moscow, Russia

[3]NILU, Department for Atmospheric & Climate Research (ATMOS), 2007 Kjeller, Norway

[4]ERL, Institute of Nuclear and Radiological Science & Technology, Energy & Safety, NCSR Demokritos, 15341 Attiki, Athens, Greece

***** Corresponding author: N. Evangeliou (Nikolaos.Evangeliou@nilu.no)

Supplementary Figures

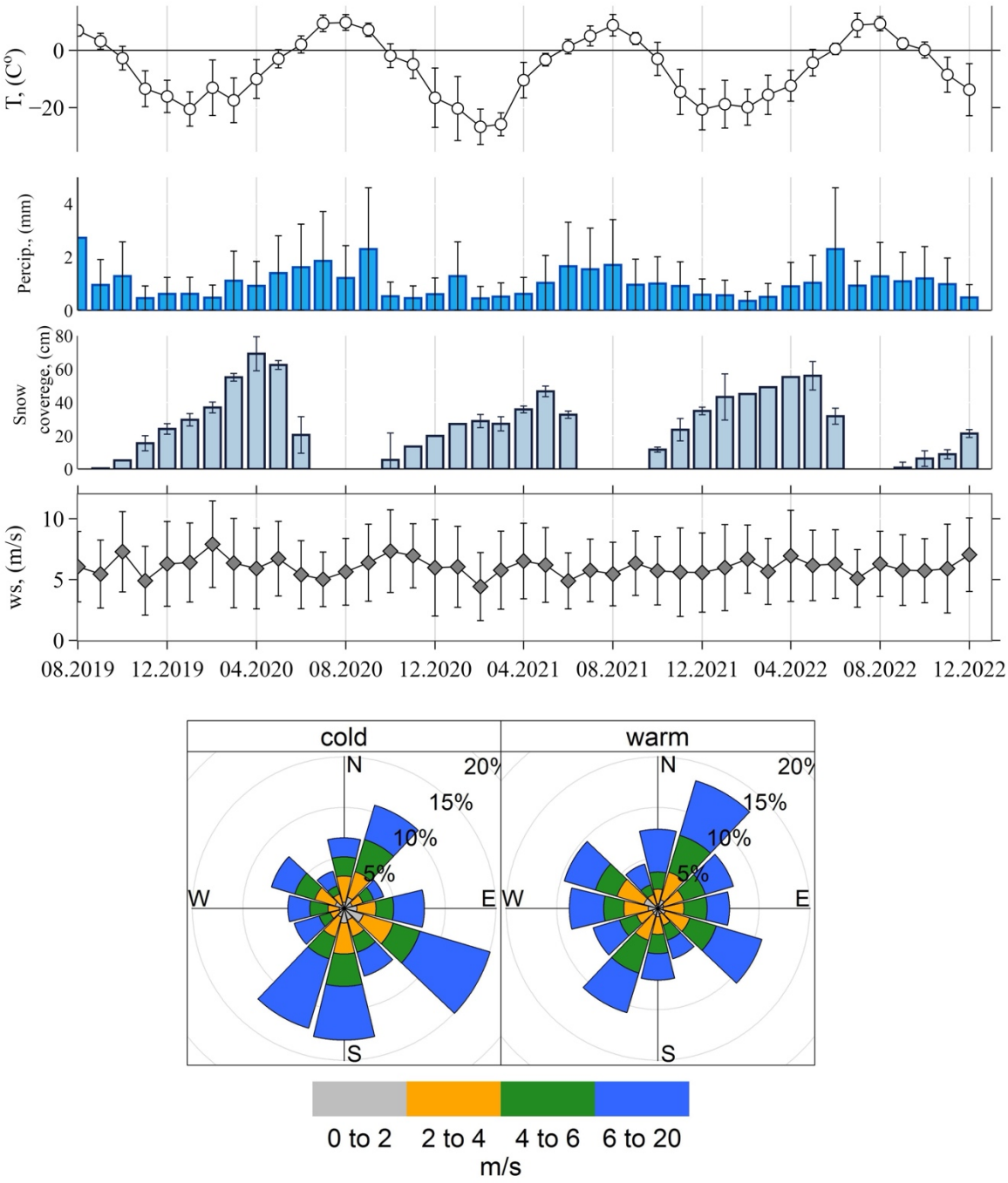

Figure S 1. (top) Monthly mean local meteorological variables: temperature, precipitation, snow coverage, and wind speed from 10 August 2019 to 31 December 2022 in the Bely Island. Standard deviations are shown with whiskers. Date format is mm.YYYY. (bottom) Wind roses for the cold and warm periods showing the prevailing wind circulation.

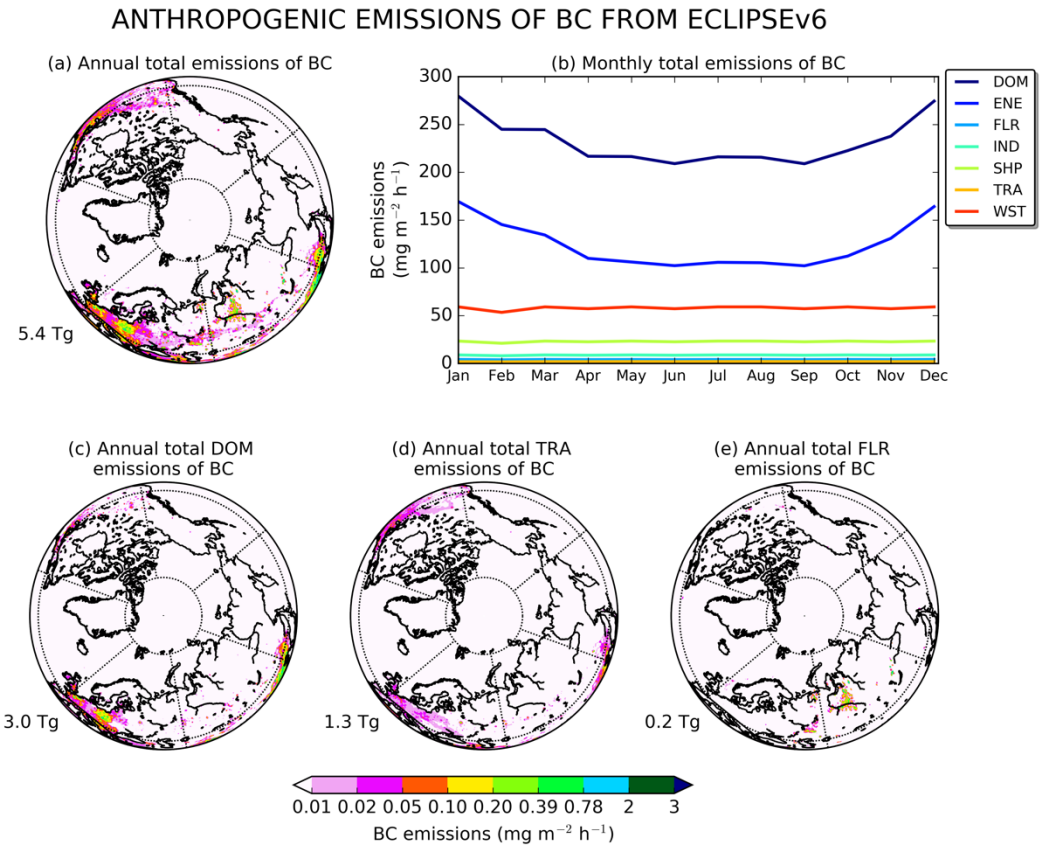

Figure S 2. (a) Annual total and (b) monthly anthropogenic BC emissions, (c) annual total domestic (DOM), (d) traffic (TRA), and (e) gas flaring (FLR) emissions of BC from ECLIPSEv6 emission inventory.

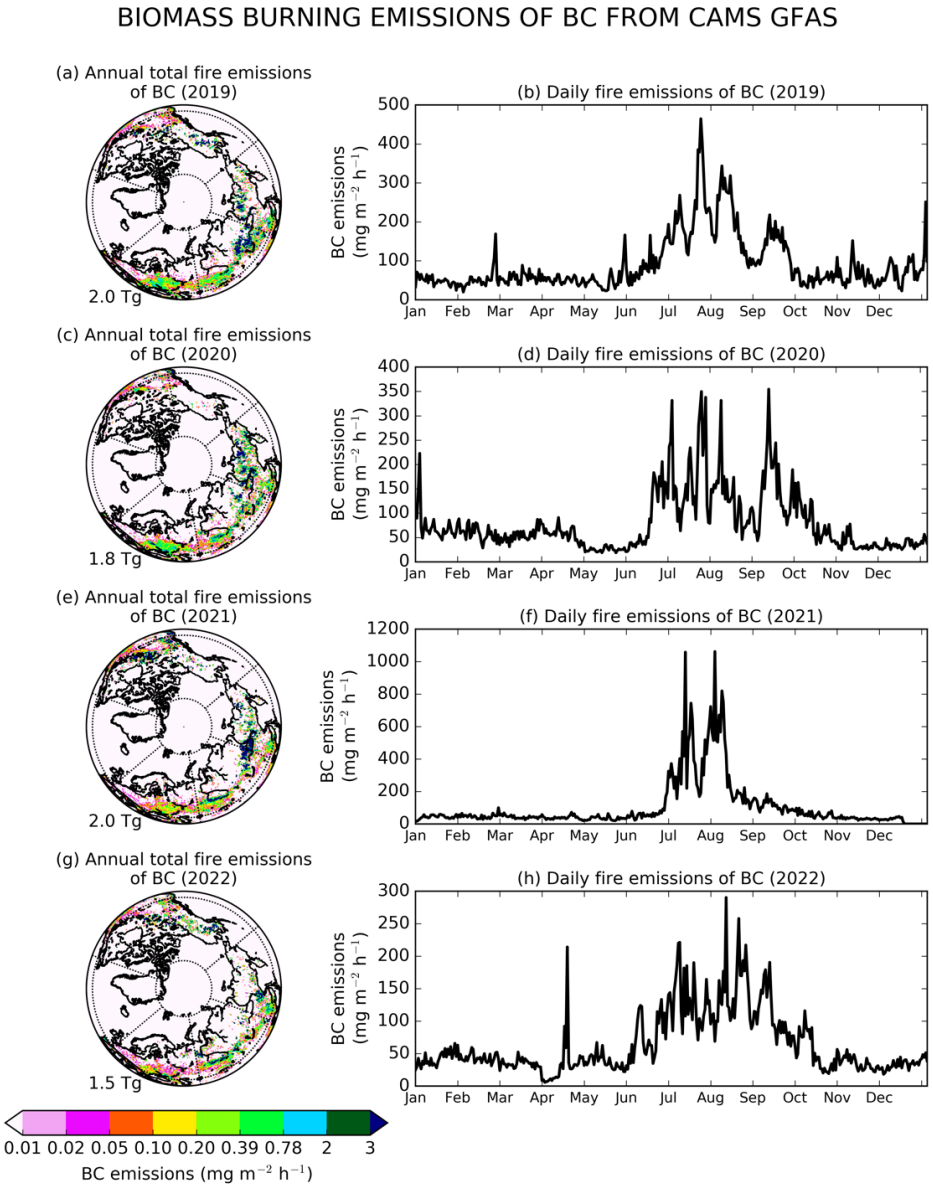

Figure S 3. Annual total and daily fire emissions of BC from the CAMS Global Fire Assimilation System (GFAS).

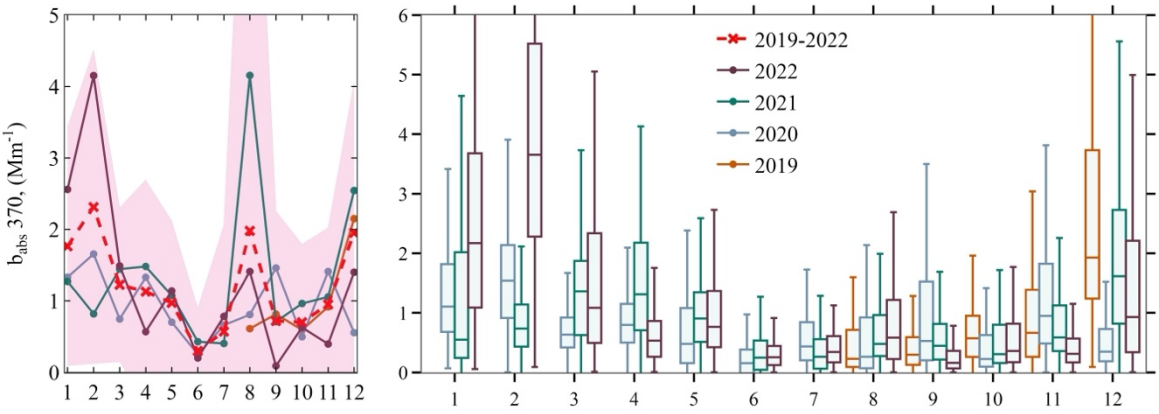

Figure S 4. Monthly means (left) and box-whisker plot (right) of babs(370). The 25th, 50th, and 75th percentiles are shown with boxes, while whiskers extend ±1.5 times the interquartile range.

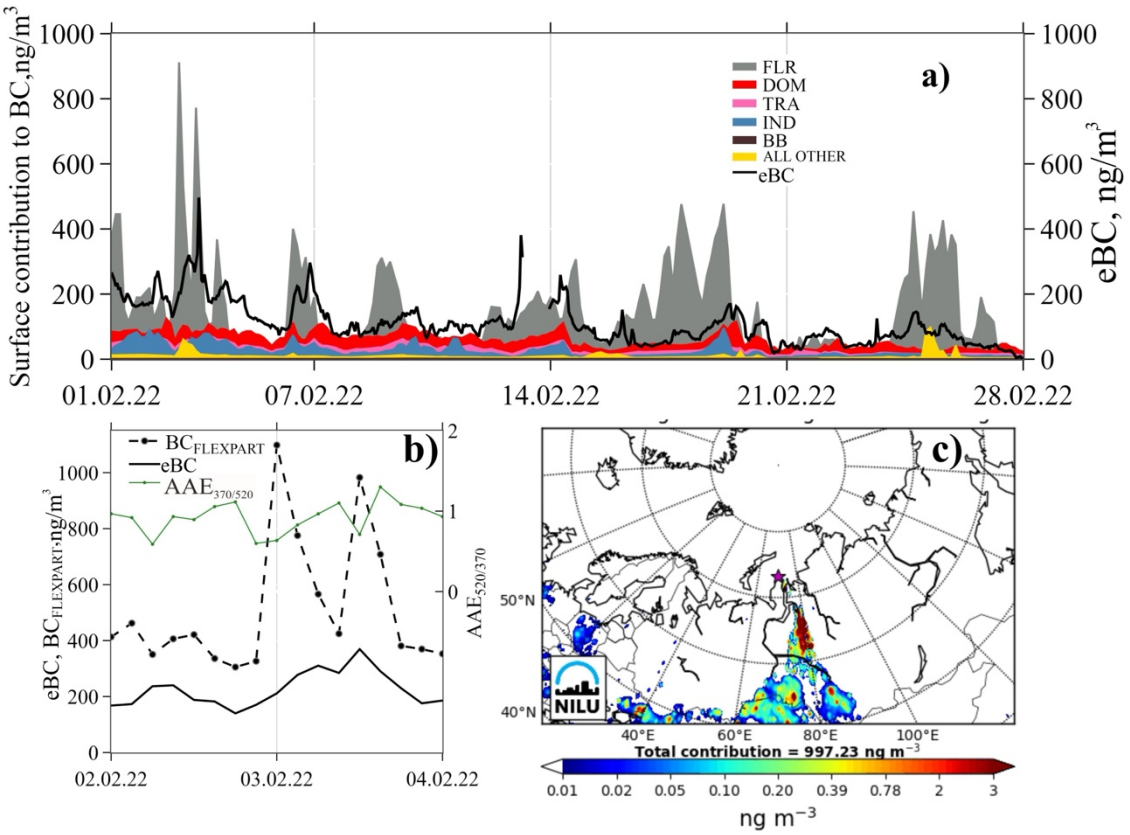

Figure S 5. (a) Time series of 3-hourly eBC concentrations and contributions from different emission source types to the BC surface concentrations during February 2021. (b) Episode of highest eBC and simulated BC, AAE370/520. (c) Spatial distribution of anthropogenic contribution to surface BC to the Island Bely station on 5 August 2021.

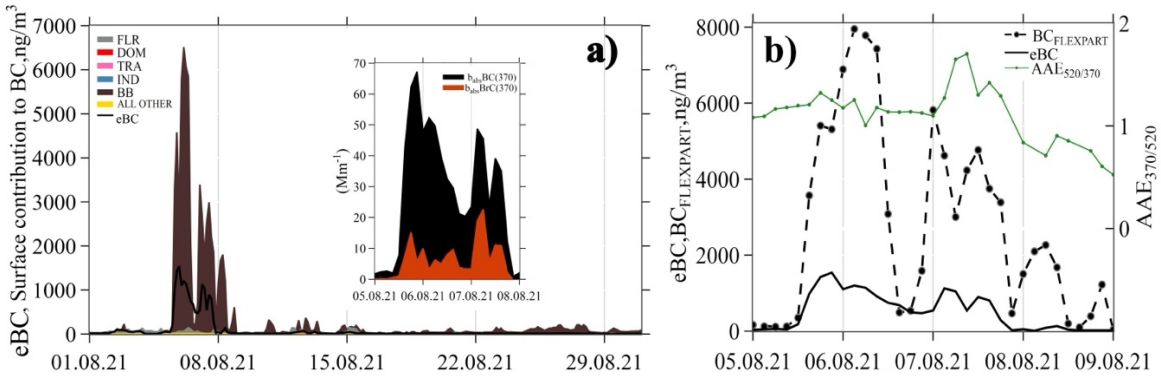

Figure S 6. (a) 3-hourly surface BC concentrations simulated with FLEXPART coupled to ECLIPSEv6-GFAS during August 2021. Contribution from different emission source types to the BC surface concentrations. (b) eBC concentrations observed at Bely and the respective AAE. The insert shows $b_{absBC}(370)$ and $b_{absBrC}(370)$.

Supplementary Tables

Table S 1. Annual average statistics (mean, standard deviation, minimum, maximum) of meteorological parameters from August 2019 to December 2022 for the Bely Island.

		mean	sd	min	max
°C	Temperature	-6,3	12,0	-39,4	23,1
m s^{-1}	Wind speed	6,0	3,1	0,0	20,0
mm Hg	Pressure	757	10	721	788
%	Relative humidity	87	8	4	100
mm	Precipitation	1,0	1,6	0,1	22
cm	Snow coverage	32	18	0,4	73

Table S 2 . Annual and monthly eBC, $AAE_{370/520}$ and $AAE_{370/950}$ statistics.

period	**eBC , ng/m^3**			**$AAE_{(370/520)}$**			**$AAE_{(370/950)}$**		
year	mean	sd	median	mean	sd	median	mean	sd	median
2019	33	44	16	1.0	1.5	0.9	0.9	0.6	0.9
2020	24	29	15	1.0	1.6	1.0	1.0	0.6	1.0
2021	33	85	14	0.9	1.4	0.8	0.9	0.6	0.9
2022	32	48	12	1.3	1.6	1.0	1.0	0.6	1.0
month	2019								
8	10	12	5	1.5	1.8	1.4	1.1	0.7	1.1
9	14	19	7	1.2	1.7	1.1	1.0	0.7	1.0
10	19	16	14	0.8	1.2	0.8	0.8	0.5	0.8
11	29	30	19	0.8	1.4	0.7	0.9	0.6	0.8
12	81	64	58	0.7	0.8	0.7	0.9	0.3	0.9
2020									
1	35	25	30	0.8	0.9	0.9	0.9	0.4	1.0
2	41	24	39	0.9	0.7	0.9	1.0	0.3	1.0
3	22	16	19	0.8	1.1	0.7	0.9	0.5	0.9
4	31	43	18	0.7	1.5	0.7	0.9	0.6	0.9
5	18	18	12	0.9	1.9	0.9	1.0	0.8	0.9
6	8	11	5	1.5	2.4	1.5	1.1	1.0	1.0
7	14	14	9	1.4	1.9	1.4	1.1	0.7	1.2
8	19	27	6	1.3	2.0	1.3	1.0	0.8	1.0
9	31	48	13	0.9	1.7	1.0	0.9	0.7	1.0
10	14	21	7	0.9	1.7	0.9	0.9	0.7	0.9
11	35	29	27	1.0	1.0	1.0	1.0	0.4	1.0
12	15	16	9	1.1	1.5	1.1	0.9	0.6	0.9
2021									
1	35	39	13	0.8	1.0	0.9	0.9	0.4	0.9
2	24	18	16	0.9	1.1	0.8	0.9	0.4	0.9
3	42	33	38	0.7	1.3	0.6	0.9	0.5	0.8
4	35	26	31	0.8	1.0	0.8	1.0	0.4	1.0
5	23	19	17	0.9	1.6	0.8	1.0	0.7	1.0
6	10	15	6	1.5	2.2	1.4	1.1	0.9	1.1
7	11	16	7	1.2	2.1	1.1	1.0	0.8	0.9
8	83	249	11	1.0	1.3	0.9	0.9	0.5	0.9
9	17	24	10	0.9	1.2	0.8	0.9	0.5	0.9
10	25	41	10	0.7	1.1	0.7	0.7	0.5	0.7
11	31	34	17	0.9	0.8	0.8	0.9	0.4	0.8
12	64	65	42	1.0	0.8	1.0	1.0	0.4	1.0
2022									
1	61	49	49	1.0	0.5	1.0	1.1	0.2	1.1
2	106	67	92	0.9	0.2	0.9	1.0	0.2	1.0
3	42	39	29	0.8	0.6	0.8	1.0	0.3	0.9
4	14	14	10	1.1	1.1	1.1	1.0	0.4	1.0
5	25	31	14	1.3	1.8	1.2	1.1	0.7	1.1
6	6	8	4	1.8	2.4	1.8	1.2	1.0	1.2
7	23	78	5	1.9	2.3	1.5	1.2	0.9	1.0
8	28	54	8	1.8	2.4	1.3	1.2	1.0	1.1
9	4	3	3	1.8	2.6	1.7	1.1	1.0	1.0
10	16	20	9	0.9	1.3	0.9	0.9	0.5	0.9
11	12	13	8	1.1	1.1	1.1	1.0	0.5	1.0
12	37	34	25	1.0	0.9	1.0	1.0	0.4	1.0

Table S 3. Monthly $b_{abcBC}(370)$ and $b_{absBrC}(370)$, and b_{absBrC} contribution to total $b_{abs}(370)$.

date	$b_{abcBC}(370)$, Mm^{-1}	$b_{absBrC}(370)$, Mm^{-1}	BrC contribution (%)
August 2019	467	9	2%
February 2020	1524	132	8%
April 2020	1286	45	3%
July 2020	600	49	7%
September 2020	1359	86	6%
November 2020	1308	102	7%
May 2021	1030	45	4%
August 2021	3594	556	13%
December 2021	2411	129	5%
January 2022	2289	264	10%
February 2022	3944	190	5%
May 2022	1068	69	6%
August 2022	1195	217	15%
December 2022	1370	28	2%

Table S 4. Annually average mean contributions from age spectrum, regions and source sectors for 2019-2022 years, cold and warm periods.

mean contributions to BC	entire period	warm period	cold period
age spectrum			
1- 3 days	31%	24%	33%
3-6 days	22%	19%	24%
6 - 9 days	16%	25%	12%
9 - 18 days	18%	16%	19%
18 - 30 days	13%	16%	12%
Regions			
Asia	7%	2%	8%
Europe	11%	6%	13%
Northern America	4%	8%	2%
EUrus/Siberia/Far East	77%	82%	74%
Other	1%	2%	2%
source sectors			
BB	3%	48%	2%
DOM	14%	5%	18%
FLR	50%	32%	59%
IND	6%	4%	7%
TRA	9%	7%	10%
Other	17%	3%	3%

Case study

The section shows the approach used to identify the event is various in different studies. During an Arctic smoke event at Zeppelin, an atypical weather pattern established a pathway for a rapid transport of BB aerosols from fires in Eastern Europe to the Arctic (Stohl et al., 2007). Pulimeno et al. (2024) focused on long-lasting events that exceeded the 50th percentile of light absorption coefficient in the reference month to differentiate extreme wildfire events from short-term variability in the measurements. Observations of AAE above 1.0 supported by chemical composition was used for characterization of the impact of North American intense fires upon the European Arctic (Markowicz et al., 2016). Popovicheva et al. (2022) assumed pollution episodes to be repeated events of eBC concentrations higher than the 80th percentile. Here, we focus on the events of the record high BC pollution level occurred at a monthly level. February 2022 was month with the highest concentrations in the cold period and August 2021 was characterised by unprecedented high smoke in the warm period; both, they are chosen for a case study here.

In February 2022, the timeseries of eBC concentration showed a high variability from 3 to 369 ng m^{-3} (**Figure S 5a**). FLEXPART overestimated surface BC values by 178 ng m^{-3}, on averag. Looking closely to specific episodes, two peaks of high eBC concentrations were observed (**Figure S 5b**). On 3 February at 12:00 to 16:00, eBC reached 310 and 369 ng m^{-3}, respectively, while FLEXPART simulated overestimated BC values of 1100 and 980 ng m^{-3} at 00:00 and 13:00 (3 February), respectively. Spatial distribution of anthropogenic contributions showed that gas flaring regions at KMAO and YNAO were the highest (**Figure S 5c**) with 54% contribution to surface BC. AAE370/520 values between 0.7 and 1.1 confirmed the anthropogenic source impact of the transported aerosols.

In August 2021, the second hottest August (14.9°C) during a 43-year NCEP-DOE reanalysis record (1979–2021) was observed in central Yakutia (Tomshin and Solovyev, 2022). Intensification of wildfires associated with positive temperature anomalies and persistent high-pressure systems promoted dry weather conditions by blocking the transport of moist air masses from the European part of Russia. Since the beginning of August the eBC concentrations at Island Bely were very low, around the arctic background defined in Popovicheva et al. (2022) as 10 ng m−3. Smoke started with a sharp increase at 9:00 on 5 August and lasted until 6:00 on 7 August (**Figure S 6**). Unprecedented high wildfire-related smoke characterized by a large peak and a long duration averaged babsBrC contribution to total babs(370) of 50% and 20% (**Figure S 6**). Calculation of babsBC and babsBrC during events shows the apparent dominance of BC absorption (**Figure S 6**). This is mainly because the mass of OC was ~35 times higher than the mass of EC. AAE370/520 approached 1.7 on 7 August (**Figure S 6**b), the characteristic of aged BB plume with elevated BrC light absorbers in transported smoke aerosols. The weekly average of AAE405/808 accounted for 1-1.2, indicating intense atmospheric aging and degradation of BrC chromophores from the wildfire plume (Schneider et al., 2024). FLEXPART model captures this event well, simulates the variability but overestimates surface BC, by up to 6200 ng m-3 at the peak value (**Figure S 6**). The reason might be use of increased emission factors for BC during Yakutian wildfires in the adopted CAMS GFAS emissions. Notably, air masses of 6-9 day aging contribute 71% whereas the shorter 3-6 days only 18%.

References

Markowicz, K.M., Pakszys, P., Ritter, C., Zielinski, T., Udisti, R., Cappelletti, D., Mazzola, M., Shiobara, M., Xian, P., Zawadzka, O., Lisok, J., Petelski, T., Makuch, P., Karasinski, G., 2016. Impact of North American intense fires on aerosol optical properties measured over the European Arctic in July 2015. J. Geophys. Res. 121, 14487–14512. https://doi.org/10.1002/2016JD025310

Popovicheva, O.B., Evangeliou, N., Kobelev, V.O., Chichaeva, M.A., Eleftheriadis, K., Gregorič, A., Kasimov, N.S., 2022. Siberian Arctic black carbon: gas flaring and wildfire impact. Atmos. Chem. Phys. 22, 5983–6000. https://doi.org/10.5194/acp-22-5983-2022

Pulimeno, S., Bruschi, F., Feltracco, M., Mazzola, M., Gilardoni, S., Crocchianti, S., Cappelletti, D., Gambaro, A., Barbaro, E., 2024. Investigating the Presence of Biomass Burning Events at Ny-Å Lesund: Optical and Chemical Insights from Summer-Fall 2019. Atmos. Environ. 320, 120336. https://doi.org/10.1016/j.atmosenv.2024.120336

Schneider, E., Czech, H., Popovicheva, O., Chichaeva, M., Kobelev, V., Kasimov, N., Minkina, T., Rüger, C.P., Zimmermann, R., 2024. Mass spectrometric analysis of unprecedented high levels of carbonaceous aerosol particles long-range transported from wildfires in the Siberian Arctic. Atmos. Chem. Phys. 24, 553–576. https://doi.org/10.5194/acp-24-553-2024

Stohl, A., Berg, T., Burkhart, J.F., Fjæraa, A.M., Forster, C., Herber, A., Hov, Ø., Lunder, C., McMillan, W.W., Oltmans, S., Shiobara, M., Simpson, D., Solberg, S., Stebel, K., Ström, J., Tørseth, K., Treffeisen, R., Virkkunen, K., Yttri, K.E., 2007. Arctic smoke – record high air pollution levels in the European Arctic due to agricultural fires in Eastern Europe in spring 2006. Atmos. Chem. Phys. 7, 511–534. https://doi.org/10.5194/acp-7-511-2007

Tomshin, O., Solovyev, V., 2022. Features of the Extreme Fire Season of 2021 in Yakutia (Eastern Siberia) and Heavy Air Pollution Caused by Biomass Burning. Remote Sens. 14. https://doi.org/10.3390/rs14194980